Role of Specific Amino Acid Residues in T4 Endonuclease V That Alter Nontarget DNA Binding†

Simon G. Nyaga, M. L. Dodson, and R. Stephen Lloyd*

Sealy Center for Molecular Science and The Department of Human Biological Chemistry and Genetics, The University of Texas Medical Branch, Galveston, Texas 77555-1071

Received August 30, 1996; Revised Manuscript Received January 22, 1997⊗

ABSTRACT: Endonuclease V is a pyrimidine dimer-specific DNA glycosylase−apurinic (AP)[1] lyase which, *in vivo* or at low salt concentrations *in vitro*, binds nontarget DNA through electrostatic interactions and remains associated with that DNA until all dimers have been recognized and incised. On the basis of the analyses of previous mutants that effect this processive nicking activity, and the recently published cocrystal structure of a catalytically deficient endonuclease V with pyrimidine dimer-containing DNA [Vassylyev, D. G., *et al*. (1995) *Cell 83*, 773−782], four site-directed mutations were created, the mutant enzymes expressed in repair-deficient *Escherichia coli*, and the enzymes purified to homogeneity. Steady-state kinetic analyses revealed that one of the mutants, Q15R, maintained an efficiency (k_{cat}/K_m) near that of the wild-type enzyme, while R117N and K86N had a 5−10-fold reduction in efficiency and K121N was reduced almost 100-fold. In addition, K121N and K86N exhibited a 3−5-fold increase in K_m, respectively. All the mutants experienced mild to severe reduction in catalytic activity (k_{cat}), with K121N being the most severely affected (35-fold reduction). Two of the mutants, K86N and K121N, showed dramatic effects in their ability to scan nontarget DNA and processively incise at pyrimidine dimers in UV-irradiated DNA. These enzymes (K86N and K121N) appeared to utilize a distributive, three-dimensional search mechanism even at low salt concentrations. Q15R and R117N displayed somewhat diminished processive nicking activities relative to that of the wild-type enzyme. These results, combined with previous analyses of other mutant enzymes and the cocrystal structure, provide a detailed architecture of endonuclease V−nontarget DNA interactions.

The exposure of DNA to ultraviolet light (UV) of short wavelength (295 nm or less) causes the formation of several biologically important photoproducts, the most prevalent of these lesions being cyclobutane pyrimidine dimers and the 6−4 dipyrimidine adducts (Taylor, 1994). Both prokaryotic and eukaryotic cells have mechanisms either for the removal of these lesions (nucleotide excision repair or enzyme-catalyzed photoreversal) or for damage avoidance (recombination). In a limited number of organisms, a base excision repair pathway also exists for initiating the removal of these lesions [reviewed by Lloyd and Linn (1993), Lloyd (1993), and Lloyd and Van Houten (1995)]. One of these base excision repair enzymes is T4 endonuclease V. It has a narrow substrate specificity for *cis*−*syn* cyclobutane pyrimidine dimers, although recent studies have shown that it can incise *trans*−*syn* dimers and Fapy A adducts at a rate approximately 1% that of the *cis*−*syn* dimer (Smith & Taylor, 1993; Dizdaroglu *et al.*, 1996). Biochemical and genetic investigations have identified the active site of endonuclease V as the α-amino group of the N-terminal threonine residue (Schrock & Lloyd, 1991, 1993; Dodson *et al*., 1993). Nucleophilic attack results in the cleavage of the glycosyl bond of the 5′-pyrimidine of the dimer, resulting in an imino intermediate. The enzyme can either dissociate, leading to an abasic site, or proceed by a β-elimination reaction to result in an α,β-unsaturated aldehyde (Dodson *et al.*, 1993, 1994).

However, prior to catalysis, it is essential for endonuclease V to locate the specific damaged site within large amounts of undamaged DNA, referred to in this paper as nontarget DNA. This problem of site-specific target location is common to many DNA interactive proteins involved in numerous cellular processes such as gene expression, genome replication, RNA transcription, restriction/modification, and DNA repair [reviewed in von Hippel and Berg (1989) and Lloyd and Van Houten (1995)]. *In vitro*, this protein−nontarget DNA interaction has been shown to be dominated by electrostatic interactions and to be sensitive to the monovalent salt concentration of the solution, such that below 40 mM the target search is processive, while at higher salt concentrations the search becomes three dimensional or distributive. The biological importance of this nontarget DNA search mechanism has been demonstrated in numerous studies in which reductions in nontarget DNA binding result in decreased abilities of these mutants to enhance UV survival in repair-deficient *Escherichia coli* (*E. coli*) (Dowd & Lloyd, 1989a,b, 1990; Nickell *et al.*, 1991, 1992; Augustine *et al.*, 1991). Insights into what residues are important in this protein−DNA interaction have come from both mutagenesis of selected basic amino acids and the solving of the crystal structure of endonuclease V (Morikawa *et al.*, 1992). The structure which was resolved at 1.6 Å revealed the existence of a number of positively charged amino acid

† This work was supported by U.S. Public Health Service Grants ES04091 and ES06676 and American Cancer Society Grant FRA 381.

* To whom correspondence should be addressed. Telephone: 409-772-2179. FAX: 409-772-1790. E-mail: rslloyd@scms.utmb.edu.

⊗ Abstract published in *Advance ACS Abstracts,* March 15, 1997.

[1] Abbreviations: AP, apurinic/apyrimidinic; UV, ultraviolet; EDTA, ethylenediaminetetraacetic acid; FPLC, fast protein liquid chromatography; SDS, sodium dodecyl sulfate; PAGE, polyacrylamide gel electrophoresis.

S0006-2960(96)02218-0 CCC: $14.00

Table 1: Summary of Endonuclease V Mutants Previously Shown To Display Altered Nontarget DNA Binding

mutant	functional effect
R3D	diminished nontarget DNA binding
R3E	AP-specific nicking and low levels of dimer-specific nicking; no enhancement in cellular survival of repair-deficient *E. coli*
R3Q	diminished nontarget DNA binding no enhancement in cellular survival of repair-deficient *E. coli*
R3K	diminished nontarget DNA binding
R3L	substantial level of *in vitro* dimer and AP-specific nicking; unable to complement repair-deficient *E. coli*
R22Q	reduced nontarget DNA binding
R26Q	unable to complement repair-deficient *E. coli*
A30K	increased electrostatic affinity for nontarget DNA
V31L	wild-type levels of apurinic DNA-specific nicking activities
N37K	
H34K	enhanced nontarget DNA binding activity
H107K	
H56Q	reduced nontarget DNA binding
H16R	enhanced nontarget DNA binding but with diminished catalytic activity

residues that lie on the internal curvature of the comma-shaped enzyme molecule. These residues also form a groove-like depression which can accommodate one strand of B-form DNA. Recently, a cocrystal structure has been solved using a catalytically incompetent form of the enzyme, complexed with dimer-containing DNA (Vassylyev *et al*., 1995). Table 1 summarizes the published data on mutants that displayed altered nontarget DNA binding. Further analyses of these data, coupled with a closer examination of the crystal structures, revealed that additional amino acid residues may be involved in nontarget DNA binding. Thus, we hypothesized that the creation of specific mutant enzymes might yield additional information on the architecture of interaction between endonuclease V and undamaged DNA.

In addition to amino acid residues that may be important for nontarget DNA binding, it should be noted that numerous basic and aromatic amino acids have also been implicated in dimer-specific binding. These include an extensive study by Doi *et al*. (1992), who demonstrated a critical binding role for R3, R22, R26, R117, and K121, and from our laboratory in which a key role in dimer-specific binding was suggested for W128, Y129, and K130 (Recinos & Lloyd, 1988; Stump & Lloyd, 1988; Lloyd & Augustine, 1989). However, the focus of this current study was to concentrate our efforts on residues which might differentially affect nontarget DNA from target DNA binding.

MATERIALS AND METHODS

Materials. Phenyl-Sepharose CL-4B, heparin Sepharose and Mono S matrices, and column chromatographic supplies were purchased from Pharmacia. Prestained protein molecular weight markers were purchased from BRL. Duplex *cis*−*syn* thymine dimer containing 12-mer and 49-mer oligonucleotides containing a site-specific *cis*−*syn* thymine dimer and its complementary oligonucleotide were generous gifts from Drs. Colin Smith and John-Stephen Taylor (Washington University, St. Louis, MO). Kodak X-ray films (X-Omat) were purchased from Amersham. [γ-^{32}P]ATP (6000 Ci/mmol) and [α-^{32}P]ATP (6000 Ci/mmol) were purchased from DuPont-NEN. Sequenase and Sequenase version 2.0 DNA sequencing kits were purchased from United States Biochemical Corp. *Eco*RI and *Cla*I restriction enzymes, T4 polynucleotide kinase, and T4 DNA ligase were purchased from New England Biolabs, Beverly, MA. pBR322 and the mutagenic oligonucleotides (23-mers) were prepared and synthesized, respectively, in the NIEHS Center Molecular Biology Core at UTMB. Oligonucleotide sizing markers (8−32 bases) were purchased from Pharmacia. Bio-Gel P-10 (90−180 μm) matrix was purchased from Bio-Rad.

Oligonucleotide Site-Directed Mutagenesis of the denV Gene. The *E. coli* strains, phage, and plasmids used in this study are described in Table 2.

The structural gene, *den*V, encoding endonuclease V and the transcription terminator sequences were previously constructed behind the $\lambda O_L P_R$ promoter in M13mp18 (Recinos & Lloyd, 1986; Recinos *et al.*, 1986). Single-stranded M13 DNA was isolated from *E. coli* strain UT481 (Zoller & Smith, 1983) that had been previously infected with M13 mp18 $O_L P_R$ *den*V. Mutagenic oligonucleotides were designed from the published *den*V sequence (Radany *et al.*, 1984; Valerie *et al.*, 1984) to alter independently the codons for amino acids at positions Q15(CAA) to R15(CGT), K121-(AAA) to N121(AAC), K86(AAG) to N86(AAC), and R117-(CGT) to N117(AAC). The full sequences of the four 23-mer oligonucleotides, designed from the *den*V sequence, with the altered codons being underlined, were as shown: (1) Q15R, 5′ C CAT TAA GTG ACG GTC AGC CAA T 3′; (2) K121N, 5′ G TTG TGC AAT GTT TTC ATC TAA A 3′; (3) R117N, 5′ T TTC ATC TAA GTT AGC TTG TGA T 3′; (4) K86N, 5′ C TGT AGT ATC GTT GAT ATT AAA A 3′.

Table 2: *E. coli*, Phage, and Plasmid Constructs Used in This Study

strain, plasmid, or phage	genotype or phenotype	source
E. coli		
UT481	Met thy Δ(Lac-pro) hsdRBamHI hsdM$^+$ supD Tn10/F′ traD36 proAB lac I^{q}zΔ M15	C. Lark, University of Utah
AB2480	*uvr*A6 *rec*A13 *arg*$^+$ *thr*-1 *leu*-6 *thi*-1 *sup*E44 *lac*Y1*gal*K2 *ara*-14 *xyl*-5 *mtl*-1 *pro*A2 *his*-4 *arg*E3 *str*-31 *tsx*-33 *sup*-37	A. Ganesan, Stanford University
HB101	F$^-$ Δ(merC-*mrr*) *leu sup*E44 *ara*14 *gal*K2 *lac*Y1 *pro*A2 *rps*L20 (*Str r*) *xyl*-5 *mtl*-1 *rec*A13	T. Wood, University of Texas Medical Branch
plasmid		
pGX2608	Amp^{r}λ $O_L P_R$ λ 45*gal*K$^+$	Genex Corp.
pGX2608-16-*den*V$^+$	Amp^{r}λ $O_L P_R$ endonuclease V$^+$ λ 45*gal*K$^+$	Lloyd laboratory
pGX2608-*den*V$^+$ Gln-15 Arg-15	Amp^{r}λ $O_L P_R$ λ 45*gal*K$^+$ endonuclease V (Arg-15)	this study
pGX2608-*den*V$^+$ Lys-121 Asn-121	Amp^{r}λ $O_L P_R$ λ 45*gal*K$^+$ endonuclease V (Asn-121)	this study
pGX2608-*den*V$^+$ Lys-86 Asn-86	Amp^{r}λ $O_L P_R$ λ 45*gal*K$^+$ endonuclease V (Asn-86)	this study
pGX2608-*den*V$^+$ Arg-117 Asn-117	Amp^{r}λ $O_L P_R$ λ 45*gal*K$^+$ endonuclease V (Asn-117)	this study
pBR322	Amp^r	Lloyd laboratory
phage		
M13mp18-$O_L P_R$ *den*V		Lloyd laboratory

The oligonucleotides were synthesized and purified as described (Lloyd *et al.*, 1986). The purified oligonucleotides were annealed as primers to the M13mp18 O_LP_R *den*V single-stranded circular DNA template and extended using Sequenase 2.0 (Zoller & Smith, 1983). The nick was subsequently sealed by T4 DNA ligase. Following the primer extension reaction, the resultant relaxed covalently closed circular DNAs were used to transform *E. coli* UT481. Plaques containing M13mp18 O_LP_R-*den*V with the desired mutations were selected by differential hybridization utilizing ^{32}P-end-labeled mutagenic oligonucleotides as probes (Benton & Davis, 1977; Recinos & Lloyd, 1986). Phage from the initial positive plaques were selected and purified. Single-stranded DNAs were prepared from second round screening of positive plaques, and the mutations were confirmed by DNA sequence analysis (Sanger *et al.*, 1977).

Double-stranded replicative form (RF) M13mp18 DNAs containing the desired mutations were isolated (Zoller & Smith, 1983) and the mutant *den*V genes liberated by a *Cla*I restriction digestion. These fragments were subcloned into the *E. coli* expression vector pGX2608 (Recinos & Lloyd, 1986) and transformed into *E. coli* HB101. The colonies were selected by ampicillin resistance and differential hybridization using a *den*V gene-specific probe. Plasmid DNAs were prepared from the positive colonies, and the correct orientation of the *den*V fragments was confirmed by diagnostic restriction digestions with *Eco*RI and *Cla*I (Recinos & Lloyd, 1986). Plasmids containing the wild-type and the mutant *den*V genes in the correct orientation were transformed into the recombination and excision repair-deficient *E. coli* AB2480 (*uvrA*$^-$, *recA*$^-$) and used for establishing cultures (inoculation) for protein purification.

Intracellular Accumulation of the Mutant Endonuclease V Proteins. *E. coli* AB2480 strains containing the plasmids encoding the wild-type and mutated *den*V genes were grown to stationary phase at 30 °C in Luria−Bertani (LB) medium supplemented with 100 μg/mL ampicillin (Recinos & Lloyd, 1986). The cells were harvested, resuspended at a constant optical density, and analyzed for the accumulation of immunoreactive endonuclease V by SDS−PAGE and subsequent Western blot analyses (Laemmli, 1970; Towbin *et al.*, 1979; Burnette, 1981; Higgins & Lloyd, 1987).

Mutant Protein Purification. The wild-type and mutant proteins were expressed in *E. coli* AB2480 utilizing the λO_LP_R hybrid promoter within the pGX2608. Cultures of each mutant (3 L) were grown at 30 °C for 16 h in LB broth media supplemented with 100 μg/mL ampicillin. Approximately 3×10^{12} cells were pelleted by centrifugation at 7000 rpm for 10 min at 4 °C and resuspended in 240 mL of 20 mM Tris-HCl (pH 7.5), 10 mM EDTA, 200 mM potassium chloride, and 10% (v/v) ethylene glycol (buffer A). The resuspended cells were then lysed by sonication (Branson Sonifier 450, Danbury, CT), and the cellular debris was removed by centrifugation in a Sorvall GSA rotor (10 000 rpm for 20 min at 4 °C). Complete cell lysis was confirmed by examination of samples before and after sonication using a light microscope (Zeiss, Thornwood, NY).

The supernatant was passed through a 500 mL single-stranded DNA−agarose column (Schaller *et al.*, 1972) that was equilibrated with buffer A. After the column was extensively washed, the bound proteins were eluted with a continuous salt gradient starting with buffer A to buffer A supplemented with 1.5 M potassium chloride (buffer B). This was followed by a 500 mL wash with buffer B. The fractions were monitored for the presence of mutant endonuclease V by Coomassie brilliant blue staining, silver staining, and Western blot analyses. The fractions containing the highest concentrations of mutant endonuclease V proteins were pooled. Saturated ammonium sulfate was added to a final concentration of 700 mM.

The samples were then applied to a 20 mL phenyl-Sepharose column which had been equilibrated with excess 25 mM sodium phosphate (pH 6.8), 1.0 mM EDTA, 10% (v/v) ethylene glycol, and 700 mM ammonium sulfate (buffer C). The bound proteins were washed with approximately 150 mL of buffer C. A continuous salt gradient starting with buffer C to buffer C without ammonium sulfate (buffer D) was used to elute the bound proteins. The flow through and sample fractions were monitored as described above. Wild-type and all mutant proteins eluted in the flow through.

These fractions were dialyzed against three buffer changes at 4 °C with buffer consisting of 25 mM sodium phosphate (pH 6.8), 1 mM EDTA (pH 8.0), and 10% (v/v) ethylene glycol (buffer E). These samples were applied to a 50 mL Mono S column (FPLC) that had been previously equilibrated with buffer E. After the column was washed with buffer E, a continuous salt gradient starting with buffer E to buffer E supplemented with 1.0 M potassium chloride (buffer F) was run, and 2.0 mL fractions were collected. The flow through and fractions were assayed for nicking activity using a duplex 5′-end-labeled 49-mer oligonucleotide containing a *cis*−*syn* pyrimidine dimer. The purity of the fractions was determined by silver staining of SDS−polyacrylamide gels.

The fractions containing the highest concentration of mutant endonuclease V were pooled and dialyzed as previously described. The proteins were applied to a 20 mL heparin−Sepharose column which had previously been equilibrated with buffer E. The column was washed with buffer E, and the bound proteins eluted by a continuous salt gradient starting with buffer E to buffer E supplemented with 1.5 M sodium chloride (buffer G). The column was washed with buffer G. Fractions (5−8 mL) were collected and assayed for activity and purity as described earlier. One of the mutants, K86N, was further purified using a Bio-Gel size exclusion matrix P-10 gel (Bio-Rad). The mutant enzyme was extensively dialyzed as described earlier and passed through a P-10 gel column (5 cm × 1 cm) which had previously been equilibrated with buffer E. Fractions (2 mL) were collected and assayed for purity and activity by silver staining of SDS−polyacrylamide gels and pyrimidine dimer nicking of a duplex 5′-end-labeled 49-mer oligonucleotide, respectively.

Pyrimidine Dimer Nicking Activities of the Mutants on 49-mer. Pyrimidine dimer-specific nicking activities of the enzymes were assayed using a duplex 49-mer oligonucleotide containing a *cis*−*syn* cyclobutane pyrimidine dimer. The 49-mer oligonucleotide (single stranded) had the sequence 5′ AGCTACCATGCCTGCACGAA**TT**AAGCAATTCGTAATCATGGTCATATGGTCATAGCT 3′ in which the two boldfaced T's (**TT**) represent the site of the *cis*−*syn* cyclobutane pyrimidine dimer. Approximately 0.3 ng of the 49-mer oligonucleotide was labeled on the 5′ end, using [γ-^{32}P]ATP, and annealed to an excess of the complementary oligonucleotide. The oligonucleotide was incubated at 37 °C with increasing concentrations of the mutant and the wild-type enzymes in high salt buffer [25 mM sodium phosphate

(pH 6.8), 1 mM EDTA, 100 mM NaCl, and 100 μg/mL BSA]. The reactions were stopped with the addition of oligonucleotide loading buffer [95% (v/v) formamide, 20 mM EDTA, 0.02% (w/v) bromphenol blue, and 0.02% (w/v) xylene cyanol]. The products were separated on a 15% polyacrylamide gel by electrophoresis for 4 h at 800 V. The amounts of the nicked products were determined by PhosphorImager analyses (Molecular Dynamics, Sunnyvale, CA).

Steady-State Kinetics of Pyrimidine Dimer DNA Glycosylase for Wild-Type and Mutant Endonuclease V. A 12-mer oligonucleotide (substrate) with the sequence 5′ GCAC-GAA**TT**AAG 3′ (bases in boldface represent the position of the thymine dimer) which was annealed to its complement was used for these analyses. The oligonucleotide was labeled on the 5′ end with [γ-^{32}P]ATP using T4 polynucleotide kinase. The short length of these oligonucleotides and the presence of the cyclobutane pyrimidine dimer mandated experimentation to determine the maximum temperature at which the DNA was maintained as a duplex molecule.

The temperature which did not allow denaturation of the 12-mer oligonucleotide was determined as follows: 4 nM (22.4 μL) 5′-end-labeled duplex 12-mer was preincubated for a minimum of 30 min at various temperatures (10, 15, 20, and 25 °C) in buffer containing 25 mM sodium phosphate (pH 6.8), 1 mM EDTA, 100 mM NaCl, 100 μg/mL BSA, and 5% (v/v) glycerol. Wild-type endonuclease V (20 pM) was added to a total reaction volume of 280 μL and incubation allowed to continue at the respective temperatures. Aliquots (40 μL), were taken at various time points, 0 (before addition of the enzyme), 3, 6, 9, 12, and 15 min. The aliquots were added to tubes containing 0.4 μL of 10% (w/v) SDS and 1 μL of 1 M piperidine. The tubes were placed in a dry ice−ethanol bath and then heated to 90 °C for 30 min. Piperidine treatment ensured that all the AP sites were converted to single-strand breaks. The products were separated by electrophoresis through polyacrylamide gels containing 8 M urea and the products quantitated by PhosphorImager analyses. The initial rates were determined graphically from the slopes of the kinetic data. The natural logarithms of the initial rates for the different temperatures plotted against the reciprocal of the absolute temperature (K) yielded the Arrhenius plot (see Figure 2).

Various concentrations of the 12-mer oligonucleotide ranging from 1 to 50 nM were incubated at 15 °C separately with limiting concentrations of wild-type or mutant endonuclease V (see Table 3) in the presence of 5% (v/v) glycerol in a total reaction volume of 280 μL. Preincubation was done at 15 °C for a minimum of 30 min in the absence of the enzymes. The reactions were carried out in buffer containing 25 mM sodium phosphate (pH 6.8), 1 mM EDTA, 100 mM NaCl, and 100 μg/mL BSA. Aliquots (40 μL) were taken at different time points, 0, 3, 6, 9, 12, and 15 min. The reactions were terminated by the addition of 0.4 μL of 10% (w/v) SDS and 1 μL of 1 M piperidine. The tubes were placed in a dry ice−ethanol bath and then heated to 90 °C for 30 min. The samples were spun, and an equal volume of oligonucleotide loading buffer was added. The products were separated through a 15% polyacrylamide gel containing 8 M urea. Electrophoresis was carried out at constant voltage (800 V) for 3−4 h. The wet gels were exposed and analyzed by PhosphorImager. V_{max} and K_m for the wild-type and the mutant enzymes were obtained from Lineweaver−Burk plots. Previously, we have shown that this preparation of wild-type endonuclease V contains 50% active molecules based on sodium borohydride trapping experiments (McCullough *et al.*, 1996). All mutants were assumed to be 100% active, and thus the kinetic parameters reported represent minimal values.

Pyrimidine Dimer-Specific Plasmid Nicking Assay. Form I pBR322 DNA, 120 μL (500 μg/mL), in buffer containing 25 mM sodium phosphate (pH 6.8) and 1 mM EDTA was diluted to 100 μg/mL in either low salt buffer [25 mM sodium phosphate (pH 6.8), 1 mM EDTA, 100 μg/mL BSA] or high salt buffer [25 mM sodium phosphate (pH 6.8), 1 mM EDTA, 100 mM NaCl, and 100 μg/mL BSA] to a total volume of 600 μL. The DNA was irradiated by 254 nm short-wave UV light at 100 μW/cm^2 so as to generate approximately 25 dimers per plasmid DNA (Gruskin & Lloyd, 1986). Dilutions of wild-type or mutant endonuclease V (see Figure 3 legend) were added to 3.5 μg of UV-irradiated or unirradiated pBR322 to a total reaction volume of 70 μL so as to react 0.5 μg of DNA per time point. Incubation was carried out at 37 °C, and 10 μL aliquots were taken at 0, 1, 2.5, 5, 15, and 30 min. The reactions were stopped by the addition of an equal volume of electrophoresis loading buffer [50 mM Tris-HCl (pH 8.0), 40% (w/v) sucrose, 20 mM EDTA, 2% (w/v) SDS, and 0.02% (w/v) bromphenol blue]. The various forms of DNA were separated by electrophoresis through 1% agarose gels. The gels were stained with ethidium bromide and the band images captured and analyzed by the VISAGE Bioimage electrophoresis gel analysis system (Bio Image, Ann Arbor, MI). Correction for the decreased intercalation of ethidium bromide in form I DNA was accomplished by multiplying the integrated optical density (IOD) values for form I DNA by a factor of 1.42 (Lloyd *et al.*, 1978). In control experiments in which irradiated plasmid DNAs were incubated with wild-type or mutant enzymes, less than 2% conversion of form I to form II DNA was observed with no conversion to form III DNA. The small amount of nicking is likely to arise due to apurinic sites in the form I plasmid preparation.

Electrostatic Potentials for Wild-Type and Mutant Forms of T4 Endonuclease V. Mutant enzyme structures were modeled on the wild-type enzyme using the Look program (Molecular Applications Group). Electrostatic potentials at the molecular surface were calculated and displayed with GRASP (Nicholls *et al.*, 1991).

RESULTS AND DISCUSSION

Intracellular Accumulation and Purification of the Wild-Type and Mutant Endonuclease V Proteins. In order to ensure that the expression of mutant proteins did not affect the intracellular accumulation, the steady-state intracellular levels of the wild-type enzyme and each mutant enzyme were compared using SDS−polyacrylamide gel electrophoresis and Western blot analyses of crude cell lysates (Figure 1A). K86N (lane 2), R117N (lane 3), and K121N (lane 4) accumulated to levels comparable to wild type (lane 6), while Q15R (lane 5) accumulated poorly (lane 6). Lane 1 contains the negative control (pGX2608-*den*V$^-$), and therefore, no endonuclease V was present. Other transformations of the Q15R mutant into *E. coli* AB2480 (*uvrA*$^-$ *recA*$^-$) resulted in relatively higher accumulation (data not shown).

The wild-type and the mutant enzymes were purified by five chromatographic steps: single-stranded DNA−agarose, phenyl-Sepharose, Mono S (FPLC), heparin−Sepharose and

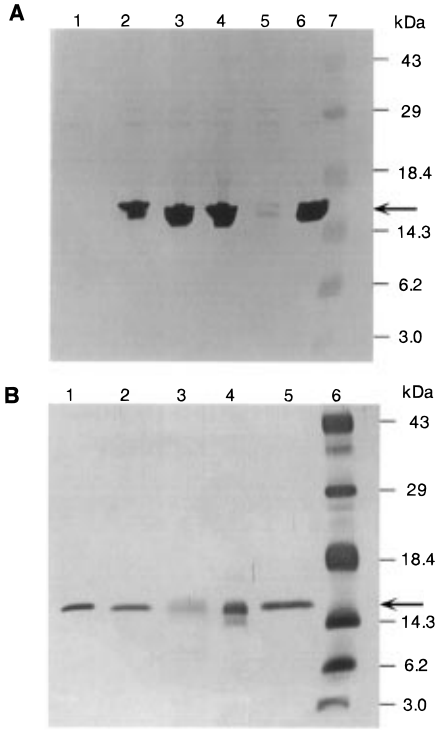

FIGURE 1: (A) Western blot analyses of endonuclease V proteins. Total cellular proteins were accumulated within the stationary phase *E. coli* AB2480 (*uvrA*$^-$ *recA*$^-$) grown at 30 °C. Samples (50 μL) of crude lysates (1.0 mg/mL) in 10 mM Tris-HCl (pH 8.0) and 1 mM EDTA were boiled in an SDS-containing buffer for 5 min before being loaded and separated by SDS−PAGE. The lane assignments are as follows: (1) pGX2608-*den*V$^-$, (2) K86N, (3) R117N, (4) K121N, (5) Q15R, (6) wild type, and (7) prestained molecular mass markers. The arrow shows the positions of wild-type or mutant forms of endonuclease V. (B) Silver staining of wild-type and mutant endonuclease V. Purified wild-type and mutant endonuclease V (20−50 μL) was mixed with an equal volume of SDS loading buffer. The samples were boiled for 5−10 min and then separated by SDS−PAGE. The proteins were stained by silver salts. Lanes: (1) WT endonuclease V, (2) K86N, (3) R117N, (4) K121N, (5) Q15R, and (6) molecular mass markers. The arrow shows the positions of wild-type or mutant forms of endonuclease V.

Bio-Gel P-10. All the proteins were purified to apparent homogeneity as revealed by silver staining of SDS−polyacrylamide gel (Figure 1B). The proteins were determined to be catalytically active by the ability to nick a duplex 49-mer oligonucleotide containing a *cis*−*syn* cyclobutane pyrimidine dimer (data not shown). The final protein concentrations were determined to be as follows: wild type, 40 nmol/mL; Q15R, 20 pmol/mL; R117N, 650 pmol/mL; K86N, 20 pmol/mL; and K121N, 93 pmol/mL.

Steady-State Kinetics of Pyrimidine Dimer DNA Glycosylase for Wild-Type and Mutant Endonuclease V. In order to determine the basic steady-state kinetic parameters for all of the purified enzymes, we chose to use a short, 12-mer oligonucleotide that contained a single site-specific cyclobutane pyrimidine dimer. This oligonucleotide was constructed by J. S. Taylor at Washington University and was designed on the basis of the footprint of endonuclease V on a 49-mer substrate that also contained a site-specific dimer (Latham *et al*., 1995). Those experiments revealed an asymmetric positioning of the dimer within the footprint. Due to both the short length of the substrate and the presence of the dimer lesion, we first needed to establish the appropriate conditions under which the 12-mer remained duplex.

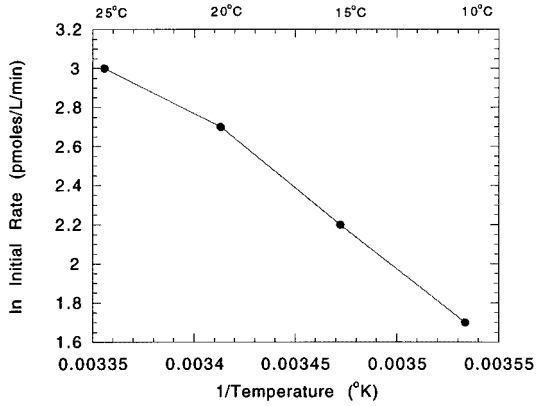

FIGURE 2: Arrhenius plot for wild-type endonuclease V. A duplex 5′-end-labeled 12-mer oligonucleotide (4 nM) was preincubated at various temperatures (10, 15, 20, and 25 °C) prior to the addition of wild-type endonuclease V (20 pM). Aliquots were taken at 0 (before the addition of enzyme), 3, 6, 9, 12, and 15 min and analyzed by SDS−PAGE containing 8 M urea. The Arrhenius plot was generated from a plot of natural logarithms of the initial rates versus the reciprocal of the absolute temperature (K).

Table 3: Steady-State Kinetics of Pyrimidine Dimer DNA Glycosylase for Wild-Type and Mutant Endonuclease V

	K_m (nM)	k_{cat} (min^{-1})	[E]$_t$ (nM)	k_{cat}/K_m (M^{-1} s^{-1})
WT	5	0.7	0.28	2.26×10^6
Q15R	3	0.3	20	1.42×10^6
R117N	3	0.1	2.43	5.8×10^5
K86N	24	0.4	0.5	2.64×10^5
K121N	13	0.02	2.33	2.69×10^4

Reaction mixtures (without enzyme) were preincubated for at least 30 min at 10, 15, 20, and 25 °C to ensure that temperature equilibrium had been established. Endonuclease V (wild type) was added, and aliquots were taken at various times and treated with piperidine to convert all glycosylase and glycosylase−AP lyase nicked products to a uniquely sized DNA fragment. Previous reports had indicated that the glycosylase reaction was favored at low temperatures over the combined glycosylase/AP lyase reaction (Seawell *et al*., 1980). The initial rates of incision were plotted as a function of temperature (K) (Figure 2). The 10, 15, and 20 °C reactions produced a linear Arrhenius plot, while the 25 °C rate deviated significantly. These data were interpreted to mean that the duplex DNA began melting between 20 and 25 °C. Therefore, we chose to conduct all steady-state experiments at 15 °C.

Table 3 summarizes the kinetic data for wild-type and mutant endonuclease V. Q15R and R117N exhibited near wild-type K_m values whereas K121N and K86N showed a 4−8-fold increase in K_m values respectively relative to the wild type. All the mutants had decreased (2−35-fold) catalytic activities (k_{cat}) with K121N showing a considerable decrease (35-fold) relative to that of the wild type. All the mutants showed decreases (2−84-fold) in efficiencies (k_{cat}/K_m) with the most severely affected being K86N and K121N (9- and 84-fold, respectively). These data indicate the importance of K86 and K121 in both substrate binding and subsequent catalysis.

The cocrystal structure of T4 endonuclease V and its substrate (Vassylyev *et al*., 1995) revealed that the side chains of R3, H16, R117, and K121 are involved in polar interactions with the two phosphates of the pyrimidine dimer and also that K86 is involved in substrate recognition. This is

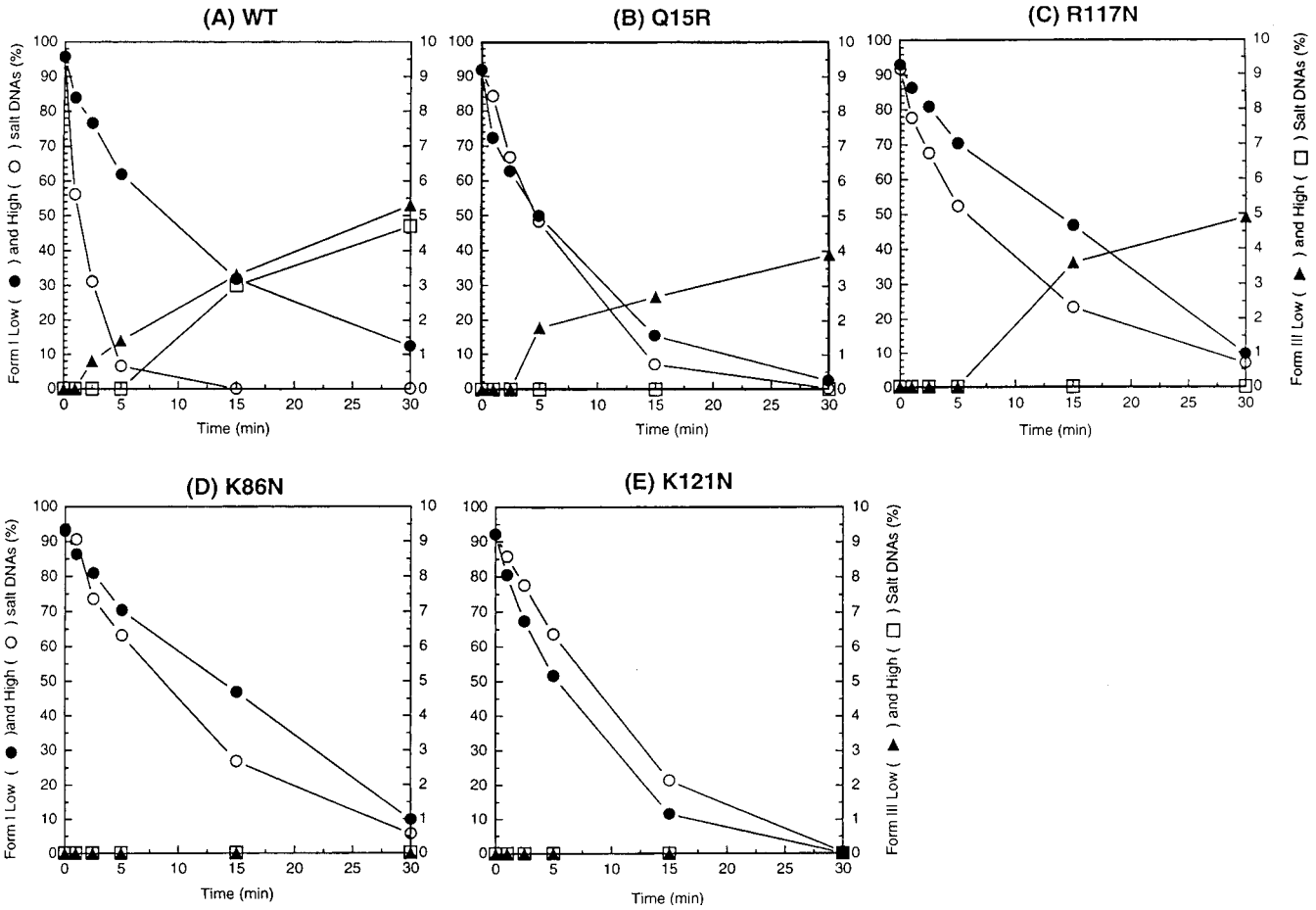

FIGURE 3: Kinetic analysis of pyrimidine dimer-specific nicking of UV-irradiated pBR322 DNA at low and high salt concentrations. pBR322 DNA containing multiple dimers per plasmid was incubated at 37 °C under low (40 mM) or high (140 mM) salt concentrations with the wild-type or mutant enzymes. Aliquots were taken at various time points (0, 1, 2.5, 5, 15, and 30 min) and analyzed for the presence of different topological DNA forms. The amounts of enzymes used were as follows: WT, 1.0 ng (low salt) and 2.5 ng (high salt); Q15R, 1.5 ng (low salt) and 1.2 ng (high salt); R117N, 12 ng (low salt) and 1.2 ng (high salt); K86N, 0.7 ng (low salt) and 1.3 ng (high salt); K121N, 30 ng (low salt) and 60 ng (high salt). The panels are as follows: (A) wild type, (B) Q15R, (C) R117N, (D) K86N, and (E) K121N. The symbols used are as follows: form I (closed circle, low salt; open circle, high salt); form III (closed triangle, low salt; open square, high salt).

consistent with decreased substrate binding of K86N and K121N, as well as the decreased catalytic activities of R117N, K86N, and K121N observed in this study. Previous studies by Doi *et al*. (1992) of R117Q and K121Q demonstrated decreased binding affinities while only K121Q showed an increased k_{cat}. The modest discrepancies observed between k_{cat} values for K121Q (Doi *et al.*, 1992) and K121N (this study) may be due to a number of factors including the lengths or conformation of the side chains of glutamine versus that of asparagine. The longer side chain of glutamine compared to that of asparagine may provide the right distance for the interaction with the phosphates of the pyrimidine dimer. The differences that are reported in k_{cat} and K_m values for wild-type endonuclease V (6-fold and 10-fold, respectively) may stem from differences in the experimental conditions by the two laboratories. In our study, a 12-mer oligonucleotide containing an asymmetrically positioned dimer was used, as opposed to a 14-mer oligonucleotide with a centrally placed dimer, and our reactions were carried out at 15 °C as opposed to 37 °C. This latter point may be especially relevant since the Arrhenius plot (Figure 2) indicated the possibility of denaturation of the 12-mer at temperatures above 20 °C.

Analyses for Processive Nicking Activity. Although the mutant enzymes showed decreased catalytic activities, it was still possible to determine whether these mutations had significantly affected nontarget DNA binding. In order to accomplish this, the processive nicking activity of endonuclease V was monitored using UV-irradiated supercoiled (form I) plasmid DNA containing multiple pyrimidine dimers per plasmid (Lloyd *et al.*, 1980). For *in vitro* analyses, low salt conditions are essential to manifest the full processivity of the wild-type enzyme, and these same conditions were used to assay the relative processivity of the altered proteins. Experimentally, when supercoiled (form I) plasmid DNA is incised, form II (nicked circular) DNA is produced, and form III (linear) DNA is generated when two nicks occur in close proximity on complementary strands. It is the rate of formation of form III DNA that is diagnostic of the processive nicking activity such that form III DNAs accumulate linearly throughout a kinetic reaction and that form I DNA is still present as form III accumulates (Lloyd *et al.*, 1980; Gruskin & Lloyd, 1986). In contrast, in analyses of reactions in which a distributive search mechanism is operational, there is a long delay in the appearance of form III DNA molecules because breaks are being put into the plasmid population on a random basis. Thus, all form I DNA disappears prior to the accumulation of significant amounts of form III DNA. The data in Figure 3 show the kinetic analyses performed at low salt conditions (closed symbols)

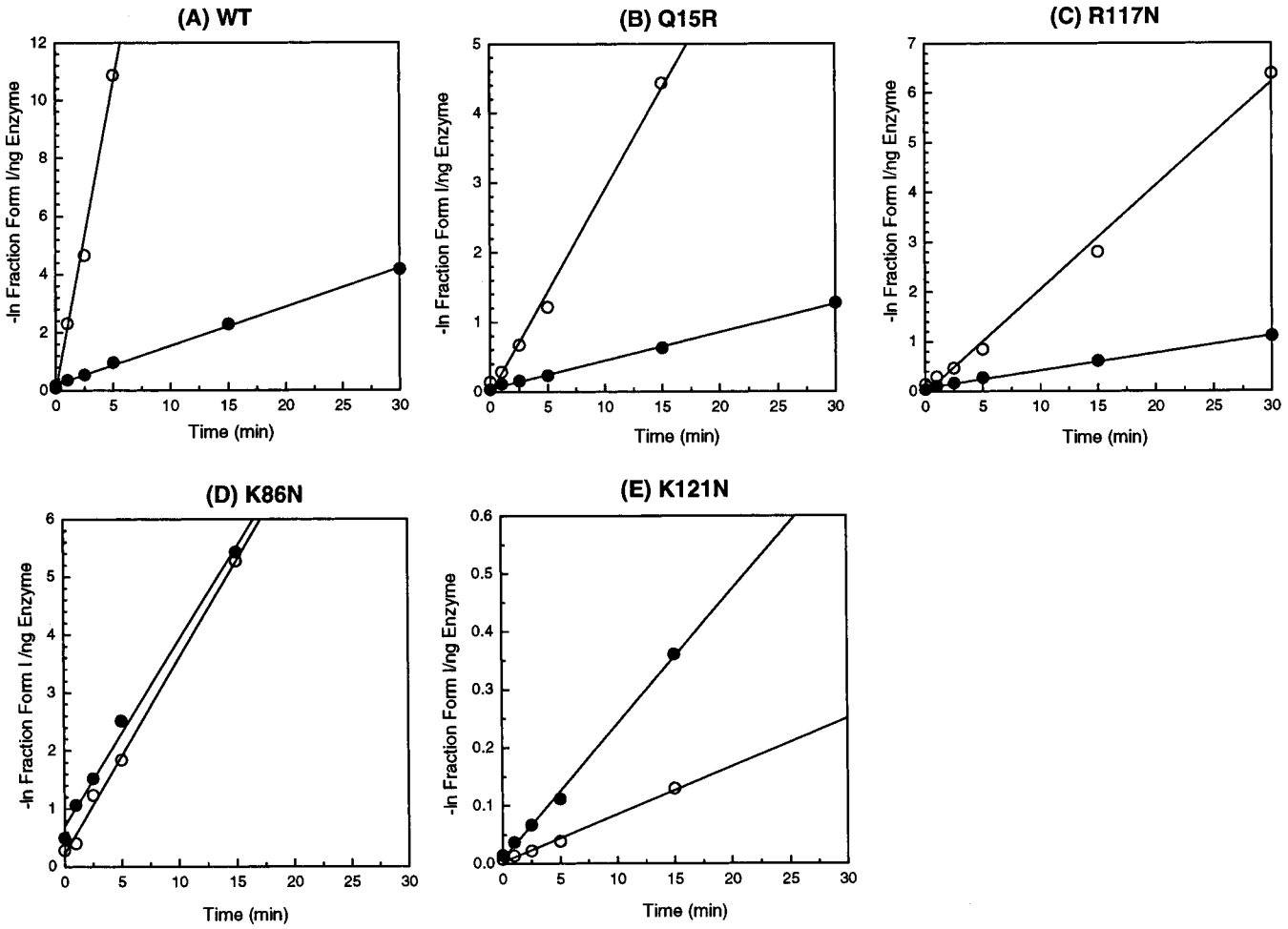

FIGURE 4: Comparative analyses of kinetic rates of incision at low and high salt concentrations. The negative natural logarithms of the mass fraction form I DNA remaining at each time point for data in Figure 3 were determined and normalized relative to the amounts of each enzyme used in each reaction. The closed circles show the dimer nicking rates obtained in low salt, while open circles show the results of dimer nicking rates in high salt conditions. Panels: (A) wild type, (B) Q15R, (C) R117N, (D) K86N, and (E) K121N.

for the wild-type enzyme (Figure 3A) and the four mutant enzymes: Q15R (Figure 3B), R117N (Figure 3C), K86N (Figure 3D), and K121N (Figure 3E).

The wild-type enzyme (Figure 3A) shows the characteristic loss in form I DNA with concomitant increases in forms II (not shown) and III. It is this linear increase in form III DNA while there is still a high percentage of form I DNA that is the hallmark of processivity (Lloyd *et al.*, 1980; Gruskin & Lloyd, 1986). The data for two of the mutants, R117N and Q15R, revealed characteristics of both processive and distributive mechanisms: evidence for processivity in that there was a significant accumulation in the percentage of form III DNA while there was still high levels of form I DNA and evidence for a distributive character in that there was a significant time lag in the appearance of the form III DNAs. Together, these data suggest that the R117N and Q15R display a limited processive nicking activity, such that dissociation occurs prior to incision of all dimers within the plasmid. These data are qualitatively similar to the incision activity of the UvrABC complex on UV-irradiated plasmid DNA, in which it was estimated that UvrABC initiates the repair over 2−3 kb segments of DNA prior to dissociation (Gruskin & Lloyd, 1988a,b).

In contrast to the two mutants described above, both the K86N and the K121N showed severe reductions in processive nicking activities, in that no form III DNAs accumulated throughout the extent of the kinetic analyses. The 30 min time point (Figure 3E) shows complete conversion of form I to form II DNA (not shown), and yet no form III DNA was present. In additional experiments, greater concentrations of these enzymes were used, and form III DNA only appeared long after the complete disappearance of form I DNAs (data not shown). Thus, we can conclude that these two mutations (K86N and K121N) have severely affected the nontarget DNA binding activity in each mutant.

To further demonstrate that each of these mutants has decreased affinity for nontarget DNA, similar reactions were carried out, except under high salt conditions (open symbols) (Figure 3). The wild-type enzyme (Figure 3A) clearly shows a distributive reaction mode in that no form III DNA accumulates until after all form I DNA has been incised. This suggests that multiple single-strand breaks were randomly introduced into the population without any significant percentage being in close proximity on complementary strands. All four of the mutants displayed complete loss of form I DNA with no increase in form III DNA, thus providing strong evidence that they also use a distributive search mechanism at high salt concentrations.

In order to assess the magnitude of the effect that changes in the salt concentration have on the processive nicking activity, a rate comparison was made for the rate of loss of form I DNA (−ln mass fraction of form I) at the two different salt concentrations. Data were normalized relative to the incision activity per nanogram of input enzyme (Figure 4

Table 4: Comparative Rates of Pyrimidine Dimer-Specific Nicking Activity

enzymes	rates of incision		ratio of incision rates, high salt/low salt	ratio relative to wild type (%)
	high salt	low salt		
WT	2.118	0.134	15.8	100
Q15R	0.292	0.041	7.1	45
R117N	0.188	0.035	5.4	33.9
K86N	0.34	0.32	1.1	7.0
K121N	0.008	0.023	0.3	1.9

and Table 4). For the wild type, a comparison of rates at the high salt versus low salt reaction conditions revealed a dramatic difference in the apparent rate of incision. However, this apparent rate difference is merely a manifestation of the wild-type enzyme's processivity, such that many breaks are put in one plasmid prior to dissociation. This interpretation is also consistent with significant accumulation of form III DNA while form I DNA was still present. Qualitatively similar data were generated for mutants Q15R and R117N in which a comparison of the −ln form I DNA is made at the high and low salt concentrations (Panels B and C of Figure 4, respectively). In contrast, the K86N (Figure 4D) mutant had identical slopes at both salt concentrations, indicating a distributive search mechanism at either salt concentration. Furthermore, the slope of the K121N was greater at low salt than at high salt (Figure 4E). These data suggest that the loss of charge at K121 severely restricts access or correct orientation of the enzyme with respect to the DNA, such that at high salt concentrations, few productive enzyme−DNA encounters occur. Thus, the rate at which single pyrimidine dimers can be located is in fact enhanced under low salt conditions. Calculations of the relative ratios of the slopes are given in Table 4. It is clear that the processivity of R117N and Q15R is close to that of the wild type while that of the K86N and K121N is very severely reduced.

Analyses of Electrostatic Potentials. In order to further understand the molecular interaction between the residues of endonuclease V and nontarget DNA, electrostatic potentials along the surfaces of wild-type and the mutant forms of endonuclease V were calculated and displayed using Graphical Representation and Analysis of Surface Properties (GRASP, Columbia University) as shown in Figure 5. In this display, the blue color represents positive charges while red represents negative charges. The R117N mutant (Figure 5C) appears to have retained wild-type electrostatic potentials (Figure 5A). The position of R117 in the cocrystal structure reveals that it is approximately in the middle of α-helix 3 as it connects the acidic face with the basic DNA interactive face (Vassylyev *et al*., 1995). Side views of the cocrystal structure reveal that it is not directly on the concave surface of the DNA interacting face, although phosphate contacts can be made through water. It is this relative position which may minimize its interaction with nontarget DNA. In addition, Q15R appears to have an increase in positive potential in the active site region (Figure 5B) as had been predicted. This may explain the wild-type activities observed in k_{cat} and K_m (Table 3) and nontarget DNA binding (Figures 3A−C and 4A−C) for both Q15R and R117N.

K121N (Figure 5E) and K86N (Figure 5D) appear to have experienced a reduction in the positive potential as shown by the distribution and the intensity of the blue color relative to that of the wild type. The distribution and intensity of the positive potential around the active site (E23 shown in red at the center of each panel in Figure 5) in the K121N mutant seem to be the most adversely affected of all the four mutants relative to the wild type. Like R117, K121 is also contained in α-helix 3 but is part of the overall basic face of endonuclease V that contacts DNA. In contrast to R117, its (K121) relative position on the positively charged face of endonuclease V readily explains the reduction in nontarget

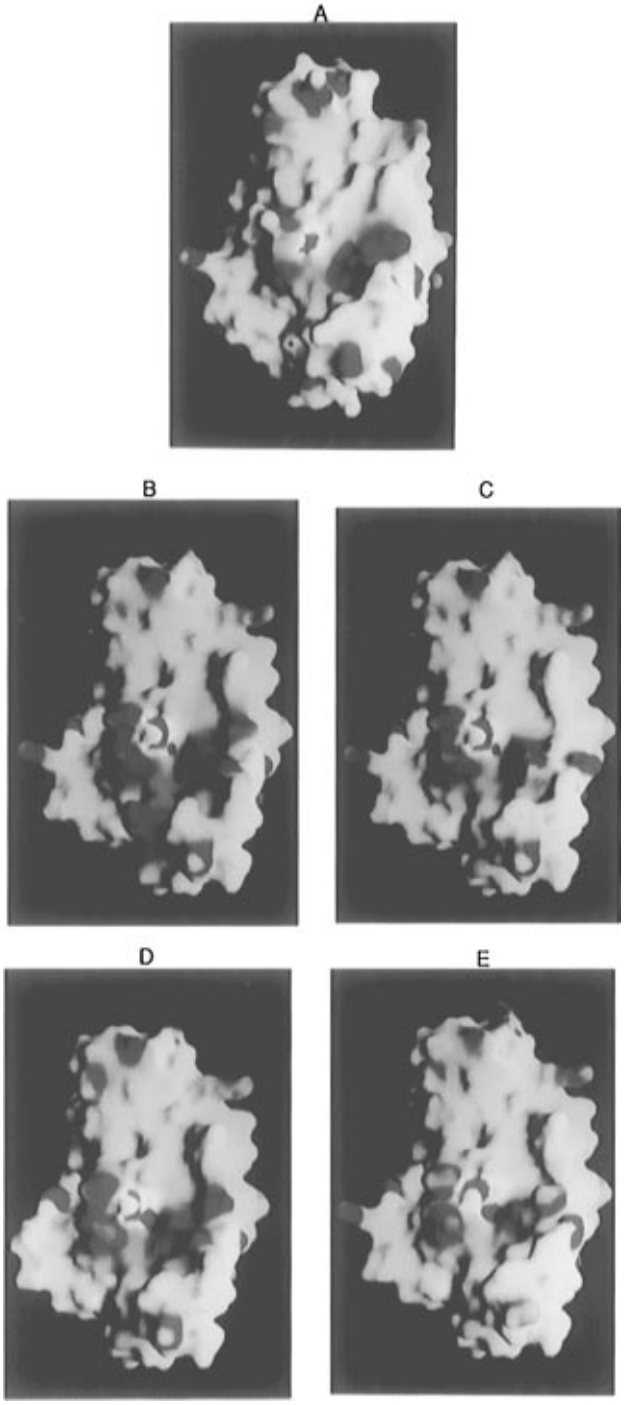

FIGURE 5: Electrostatic potentials for wild-type and mutant forms of T4 endonuclease V. Electrostatic potentials along the surfaces of both the wild-type and mutant forms of T4 endonuclease V were calculated and displayed using the GRASP program. Panels: (A) wild type, (B) Q15R, (C) R117N, (D) K86N, and (E) K121N. The color codes are blue for positive and red for negative potentials. The active site (E23) is shown as a red structure in the center of each panel.

DNA binding when its site was mutated. The K86N mutant (Figure 5D) clearly lacks a significant portion of its positive charges at the bottom left corner (position of K86). These observations may explain the reductions in k_{cat} (Table 3), increases in K_m (Table 3), and significant reductions in nontarget DNA binding (Figures 3D,E and 4D,E) for both K86N and K121N relative to that of the wild type (Table 3, Figures 3A and 4A). Our results for K86N are significantly different than those reported by Doi *et al*. (1992) in which K86 was replaced with Q86; this mutant exhibited wild-type pyrimidine dimer glycosylase activity. At the present time we do not understand the significant differences between these two mutants since both glutamine and asparagine are neutral amino acids. Additionally, inspection of the electrostatic potential reveals that the nature of the active site (E23) was not changed to any appreciable degree as shown in red at the center of each panel. This is an indication that the observed activity difference (k_{cat}, K_m, and nontarget DNA binding) between the wild type and the mutants is not likely to be due to a perturbation of the structure of the active site but rather due to the change of the nontarget DNA binding residues.

All these data, taken together, suggest that critical contact points exist between the enzyme and DNA at positions K86 and K121. Previous site-directed mutagenesis and X-ray diffraction studies have shown the critical nature of the residues at R3, R22, and R26 in nontarget DNA binding (Dowd & Lloyd, 1989a,b; Morikawa *et al*., 1992). Collectively, these data reveal that the interaction of endonuclease V with nontarget DNA is a path along the outside of the enzyme, including at least these five basic residues (R3, R22, R26, K86, and K121). These data also suggest that, for nontarget DNA interactions, there are no significant contacts made by R117 and Q15. Our previous studies also showed that another residue, K33, on the basic face of the enzyme did not make nontarget DNA contacts (Dowd & Lloyd, 1990). The steady-state kinetic results are consistent with those obtained from UV-irradiated plasmid DNAs in which K86 and K121 were residues shown to be critical in nontarget DNA binding. Thus, these studies have enabled us to have a clear understanding of the molecular interactions between endonuclease V and nontarget DNA.

ACKNOWLEDGMENT

We thank the NIEHS Center Molecular Biology Core for synthesis of the oligonucleotides. We also extend our sincere thanks to Ms. Judy Daniels for her excellent assistance in the preparation of the manuscript.

REFERENCES

Augustine, M. L., Hamilton, R. W., Dodson, M. L., & Lloyd, R. S. (1991) *Biochemistry 30*, 8052−8059.
Benton, W. D., & Davis, R. W. (1977) *Science 196*, 180−182.
Burnette, W. N. (1981) *Anal. Biochem. 112*, 195−203.
Dizdaroglu, M., Zastawny, T. H., Carmical, J. R., & Lloyd, R. S. (1996) *Mutat. Res. 362*, 1−8.
Dodson, M. L., Schrock, R. D., & Lloyd, R. S. (1993) *Biochemistry 32*, 8284−8290.
Dodson, M. L., Michaels, M. L., & Lloyd, R. S. (1994) *J. Biol. Chem. 269*, 32709−32712.
Doi, T., Recktenwald, A., Karaki, Y., Kikuchi, M., Morikawa, K., Ikehara, M., Inaoka, T., Hori, N., & Ohtsuka, E. (1992) *Proc. Natl. Acad. Sci. U.S.A. 89*, 9420−9424.
Dowd, D. R., & Lloyd, R. S. (1989a) *J. Mol. Biol. 208*, 701−707.
Dowd, D. R., & Lloyd, R. S. (1989b) *Biochemistry 28*, 8699−8705.
Dowd, D. R., & Lloyd, R. S. (1990) *J. Biol. Chem. 265*, 3424−3431.
Gruskin, E. A., & Lloyd, R. S. (1986) *J. Biol. Chem. 261*, 9607−9613.
Gruskin, E. A., & Lloyd, R. S. (1988a) *J. Biol. Chem. 263*, 12728−12737.
Gruskin, E. A., & Lloyd, R. S. (1988b) *J. Biol. Chem. 263*, 12738−12743.
Higgins, K. M., & Lloyd, R. S. (1987) *Mutat. Res. 183*, 117−121.
Laemmli, U. K. (1970) *Nature 227*, 680−685.
Latham, K. A., Taylor, J. S., & Lloyd, R. S. (1995) *J. Biol. Chem. 270*, 3765−3771.
Lloyd, R. S. (1993) in *Nucleases*, pp 445−454, Cold Spring Harbor Laboratory Press, Cold Spring Harbor, NY.
Lloyd, R. S., & Augustine, M. L. (1989) *Proteins: Struct., Funct., Genet. 6*, 128−138.
Lloyd, R. S., & Linn, S. (1993) in *Nucleases*, pp 263−316, Cold Spring Harbor Laboratory Press, Cold Spring Harbor, NY.
Lloyd, R. S., & Van Houten, B. (1995) in *DNA Repair Mechanisms: Impact on Human Diseases and Cancer* (Voss, J. M. H., Ed.) pp 25−66, Landes Co., Austin, TX.
Lloyd, R. S., Haidle, C. W., & Hewitt, R. R. (1978) *Cancer Res. 38*, 3191−3196.
Lloyd, R. S., Hanawalt, P. C., & Dodson, M. L. (1980) *Nucleic Acids Res. 8*, 5113−5127.
Lloyd, R. S., Recinos, A., III, & Wright, S. T. (1986) *Biotechniques 4*, 8−10.
McCullough, A. K., Scharer, O., Verdine, G. L., & Lloyd, R. S. (1996) *J. Biol. Chem. 271*, 32147−32152.
Morikawa, K., Matsumoto, O., Tsujimoto, M., Katayanagi, J., Ariyoshi, M., Doi, T., Ikehara, M., Inaoka, T., & Ohtsuka, E. (1992) *Science 256*, 523−526.
Nicholls, A., Sharp, K. A., & Honig, B. (1991) *Proteins 11*, 281−296.
Nickell, C., Anderson, W. F., & Lloyd, R. S. (1991) *J. Biol. Chem. 266*, 5634−5642.
Nickell, C., Prince, M. A., & Lloyd, R. S. (1992) *Biochemistry 31*, 4189−4198.
Radany, E. H., Naumovaki, L., Love, J. D., Gutekunst, K. A., Hall, D. H., & Friedberg, E. C. (1984) *J. Virol. 52*, 846−856.
Recinos, A., III, & Lloyd, R. S. (1986) *Biochem. Biophys. Res. Commun. 138*, 945−952.
Recinos, A., & Lloyd, R. S. (1988) *Biochemistry 27*, 1832−1838.
Sanger, F., Mikley, S., & Coulson, A. R. (1977) *Proc. Natl. Acad. Sci. U.S.A. 74*, 5463−5467.
Schaller, H. C., Nüsslein, F. J., Bonhoeffer, C. K., & Nietzschmann, I. (1972) *Eur. J. Biochem. 26*, 474−481.
Schrock, R. D., III, & Lloyd, R. S. (1991) *J. Biol. Chem. 266*, 17631−17639.
Schrock, R. D., III, & Lloyd, R. S. (1993) *J. Biol. Chem. 268*, 880−886.
Seawell, P. C., Smith, C. A., & Ganesan, A. K. (1980) *J. Virol. 35*, 790−797.
Smith, C. A., & Taylor, J.-S. (1993) *J. Biol. Chem. 268*, 11143−11151.
Stump, D. G., & Lloyd, R. S. (1988) *Biochemistry 27*, 1839−1843.
Taylor, J.-S. (1994) *J. Am. Chem. Soc. 27*, 76−82.
Towbin, H., Staehelin, T., & Gordon, J. (1979) *Proc. Natl. Acad. Sci. U.S.A. 76*, 4350−4354.
Valerie, K., Henderson, E. E., & deRiel, J. K. (1984) *Nucleic Acids Res. 12*, 8085−8096.
Vassylyev, D. G., Kashiwagi, T., Mikani, Y., Ariyoshi, M., Iwai, S., Ohtsuka, E., & Morikawa, K. (1995) *Cell 83*, 773−782.
von Hippel, P. H., & Berg, O. G. (1989) *J. Biol. Chem. 264*, 675−678.
Zoller, M. J., & Smith, M. (1983) *Methods Enzymol. 100*, 468−500.

BI962218X